Sarkar and Chakraborty *Geo-Engineering (2021)12:24*
https://doi.org/10.1186/s40703-021-00153-4

International Journal of Geo-Engineering

TECHNICAL NOTE Open Access

Stability analysis for two-layered slopes by using the strength reduction method

Sourav Sarkar and Manash Chakraborty*

*Correspondence: manashchakra.civ@itbhu.ac.in
Department of Civil Engineering, Indian Institute of Technology (BHU), Varanasi 221005, India

Abstract

The aim of this article is to present the slope stability charts for two layered soil slopes by using the strength reduction method (SRM). The primary focus is to provide a quantitative estimation of the improvement of slope stability when a stronger layer is placed over the weaker layer. The SRM carried in this work comprises a series of finite element lower bound (LB) and upper bound (UB) limit analysis in conjunction with nonlinear optimization. Unlike the limit equilibrium method (LEM), there is no need to consider any prior assumptions regarding the failure surface in SRM. The study is carried out for different combinations of (i) slope angles (β), (ii) strength properties of the top and the bottom layer (c, φ) and (iii) different thickness of the top layer. The failure patterns are shown for a few cases.

Keywords: Slopes, Two-layered, Stability charts, Limit analysis, SRM

Introduction

Since the last eight decades several researchers [3, 8, 12, 19, 33, 39, 44, 46] had drawn their attention for analyzing the stability of soil slopes. Nevertheless, the problem still remains to be one of the most interesting and challenging problems in geotechnical engineering. Most of the previous studies related to slope stability analysis were mainly carried out by using the limit equilibrium method (LEM). However, in LEM, prior to the analysis, shape of the slip surface, distribution of the normal stress along the slip surface and nature of the interslice forces are require to pre-assume. Moreover, strain and displacement compatibility are not being considered in LEM and hence, the method suffers serious limitations as discussed by Duncan [11] and Krahn [23]. Several other researchers [1, 2, 14, 21, 25, 32, 48, 49] used various other analytical and numerical methods for analyzing the homogenous slopes and thereby removing the limitations associated with LEM to some extent. Zaki [49] and Griffiths and Lane [15] used strength reduction method (SRM) in the framework of conventional displacement based finite element method for analyzing the homogenous slope. Yu et al. [48] and Kim et al. [21] used finite element limit analysis to analyze the homogenous slopes with and without considering the effect of pore water pressure. Michalowski [32] proposed stability charts for uniform slopes subjected to pore- water pressure and horizontal seismic force by using kinematic approach of limit analysis. Baker et al. [1] produced stability charts for homogeneous

Springer Open

© The Author(s) 2021. This article is licensed under a Creative Commons Attribution 4.0 International License, which permits use, sharing, adaptation, distribution and reproduction in any medium or format, as long as you give appropriate credit to the original author(s) and the source, provide a link to the Creative Commons licence, and indicate if changes were made. The images or other third party material in this article are included in the article's Creative Commons licence, unless indicated otherwise in a credit line to the material. If material is not included in the article's Creative Commons licence and your intended use is not permitted by statutory regulation or exceeds the permitted use, you will need to obtain permission directly from the copyright holder. To view a copy of this licence, visit http://creativecommons.org/licenses/by/4.0/.

slopes by applying the variational method and the strength reduction technique considering pseudostatic analysis.

The stability of layered slopes was also studied rigorously especially in the past few years [4, 5, 7, 17, 18, 24, 27–29, 37, 42]. By assuming the log-spiral failure mechanism, Chen et al. [7] evaluated the upper bound stability of non-homogeneous slopes corresponding to varying cohesion with depth. Kumar and Samui [24] evaluated the stability of layered soil slopes subjected to pore-water pressure and horizontal seismic force by using the rigid block upper bound limit analysis. Hammouri et al. [17] carried out the stability analysis of the layered slopes by considering the effects of rapid drawdown and tension cracks with the aid of PLAXIS 8.0 and SAS-MCT 4.0 software. By using the finite element limit analysis, [27, 28], Shiau et al. [42], and Qian et al. [37] analyzed the undrained stability of the non-homogenous cohesive soil slopes. Chang-yu et al. [18] considered rotational mechanism with logarithm helicoids surface and assessed the 3D stability of non-homogeneous slopes. Lim et al. [29] proposed stability charts for frictional fill material placed on purely cohesive soil by using finite element LB limit analysis method. By using SRM, Chatterjee and Krishna [5] analyzed two and three-layered soil slopes considering a fixed slope angle (26.57°) and different combinations of three different chosen soils. The literature review clearly indicates that the rigorous analysis for the two-layered cohesive-frictional soil slope is quite limited. Although a few stability studies [24, 38, 40, 41] were previously carried out by considering weaker layer overlying on strong layer, however, as per the authors' findings except the work of Sazzad et al. [40] hardly any study seems to be available for the case where strong layer is considered to be placed over weak stratum. The work of Sazzad et al. [40] also pertains to a specific combination of layered system (Top Soil: $c_1 = 10$ kPa, $\phi_1 = 18°$ and Bottom Soil: $c_2 = 6$ kPa, $\phi_2 = 10°$). Hence, there is a requirement to carry out an extensive and rigorous investigation to estimate the improvement in stability by placing a stronger layer over a weaker layer. This is the prime motivation to carry out the present work. In this present article, strength reduction method is employed to analyze the two-layered soil slopes and to determine the factor of safety. The factor of safety is obtained for different combinations of (i) slope geometry (i.e. slope angle, β), (ii) strength properties of the top (c_1, ϕ_1) and bottom layer (c_2, ϕ_2) (iii) and the thickness of the top layer (t). The effect of placing different stronger layers over the weaker bottom layers is thoroughly investigated.

Strength reduction method (SRM)

The work of Zienkiewicz et al. [52] appears to be the first where SRM was used to solve the slope stability problem. Following his work, many further studies [5, 9, 10, 13, 15, 16, 20, 26, 30, 31, 34, 35, 40, 45, 47, 50, 51] were performed for slope stability problems by using SRM. This method is mainly based on the frame work of finite element method (FEM) and hence, all the advantages of FEM are retained in this method. The significant advantages of this method are the following: (i) the method is suitable to apply for complex geometries, complicated boundary and loading conditions, and (ii) there is no need to consider any assumptions regarding interslice shear forces and the critical failure surface. The critical failure surface is obtained automatically from the shear strength reduction. The additional information regarding stresses, strains, and pore pressures can also be obtained from this method. SRM is also applied on the basis of finite difference

method [10]. Generally, SRM is applied to determine the factor of safety by successively reducing or increasing the shear strength of the material until the slope reaches the limiting equilibrium state.

The SRM is commonly used with the linear Mohr–Coulomb criterion where the failure strength is characterized by cohesion (c) and the internal friction angle (ϕ). The Mohr–Coulomb model is expressed in Eq. (1).

$$\tau = c + \sigma_n \tan\phi \tag{1}$$

where τ is the maximum amount of shear stress the soil can resist for a certain applied normal stress (σ_n). The analysis is carried out by reducing the strength parameters (c,ϕ) progressively until the slope becomes unstable. In conventional SRM, both parameters are reduced by the same factor, or in other words, the reduction path of the cohesion and the friction are identical. The reduced cohesion and the friction angle are computed from Eq. (2).

$$c_r = \frac{c}{F_s}\ ;\ \tan\phi_r = \frac{\tan\phi}{F_s} \tag{2}$$

where (i) c_r and ϕ_r are the reduced strength parameters and (ii) F_s is the strength reduction factor. These reduced parameters are then reinserted into the model till the failure occurs. The main objective of SRM approach is to compute the strength reduction factor and the reduced material parameters that lead to collapse state.

In the present analysis, Optum G2 [36] is used for estimating the factor of safety of the slope through strength reduction method. OptumG2 is a finite element limit analysis (FELA) based software developed by OptumCE. For obtaining the limiting solutions, OptumG2 uses second order cone programming to solve the plane-strain stability problems. This scheme works by infeasibility detection in a very controllable way [22, 43]. Following steps are adopted for the formulation:

Step 1: Assuming F_{min} and F_{max}; where, F_{min} and F_{max} are the minimum and maximum value of factor of safety. Generally, F_{min} is chosen to be zero and F_{max} is taken to be a large number within the range of machine precision.
Step 2: Initializing the value of F_s and computing reduced strength parameters with the help of Eq. (2).
Step 3: Checking feasibility through the interior point method by using the reduced strength parameters.
Step 4: If the problem is feasible, assign $F_{min}=F_S$ and evaluate a new factor of safety by using the harmonic mean as depicted in Eq. (3).

$$F_s = \left[\frac{1}{2}\left(\frac{F_{\min}F_{\max}}{F_{\min}+F_{\max}}\right)\right] \tag{3}$$

Otherwise, if the problem is infeasible, assign $F_{max}=F_S$ and evaluate a new factor of safety by following the arithmetic mean as expressed in Eq. (4).

$$F_s = \frac{1}{2}(F_{\min}+F_{\max}) \tag{4}$$

Step 5: Continue the iterative process (Step 1–Step 4) until the following convergence condition as mentioned in Eq. (5) is fulfilled:

$$\frac{F_{\max} - F_{\min}}{F_s} < T_L \tag{5}$$

here, the tolerance limit, T_L, is kept as 0·01.

It is worth mentioning that based on the solution process, F_{min} and F_{max} provides the limiting extremities of the bound theorem. F_{min} and F_{max} represent rigorous lower and upper bound on the factor of safety corresponding to the statically admissible stress field domain and kinematically admissible velocity field domain, respectively. The numerical values presented herein are the average of both the limiting values.

Problem statement and methodology

Figure 1 shows a two-layered soil slope having an angle, β. The strength parameters of the top and the bottom layer are represented by c_1, ϕ_1 and c_2, ϕ_2, respectively. Slope height (H) in the present analysis is taken as 20 m for representing the high cut slopes. With the aid of strength reduction method, it is intended to analyze and subsequently compute the factor of safety for three different two-layered slopes (namely, 25°, 35° and 45°) consisting of different soil materials.

For performing the analysis, the size of the domain is considered adequately high so that the failure surface remains contained well within the domain. Based on trials, the height (D) and length (L) of the domain are kept as $2H$ and $9H$, respectively. The boundary conditions are mentioned in Fig. 1. Vertical and horizontal displacements are restrained along the base of the considered domain. Along the left and right boundaries, horizontal displacement is not allowed to occur. The soil mass is discretized by using three nodded linear triangular elements. The soil plasticity is governed by the Mohr–Coulomb failure criterion and associated flow rule. Adaptive mesh refinement based on plastic shear dissipation has been used. Three iterations of adaptive meshing with 10,000 elements have been considered for all analyses. A nonlinear optimizer named sonic is used in Optum G2 software for optimization.

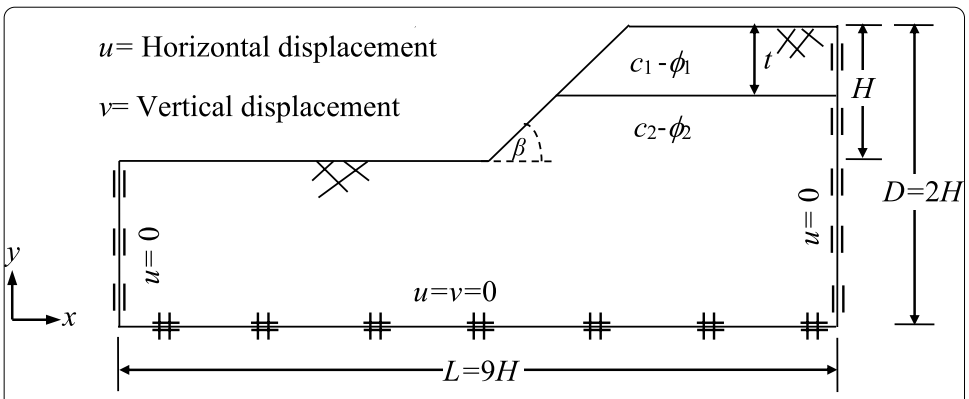

Fig. 1 Schematic diagram and the boundary conditions of a two-layered soil slope

Results and discussions

In the present work, solutions are presented in terms of factor of safety for different combinations of the (a) slope angles (β), (b) soil strength properties of the top and the bottom layers (c_1, ϕ_1 and c_2, ϕ_2) and (c) top layer thickness (t). Stability charts are presented in tabular form. Tables 1, 2, 3 show the factor of safety values computed for three different two-layered slopes ($\beta = 25°$, 35° and 45°). In this article, nine different stronger soil layers [(35,0), (35,5), (35,8), (40,0), (40,5), (40,8), (45,0), (45,5), (45,8)] were considered to be placed over twelve different weaker bottom layer [(20,5), (20,10), (20,15), (20,20), (25,5), (25,10), (25,15), (25,20), (30,5), (30,10), (30,15), (30,20)]; the first and second part within the parenthesis indicate the frictional (in degrees) and cohesive strength (in kPa), respectively. The thickness of the stronger layer was varied between 20%–80% of the domain height. Both the limiting values (lower and upper) were obtained. A total number of 3240 computations were performed. Following observations are made from the numerical results:

(a) As expected, the factor of safety (F_s) decreases with an increase in slope angle (β). However, this decrement depends on the strength of the soil layers. For an example, as β varies from 25° to 45°, F_s reduces markedly. This reduction differs by 14% (from 53 to 39%) as the cohesive strength of the top layer, ($\phi_1 = 35°$, and, $t/D = 0.4$) which is rested upon a certain bottom layer ($c_2 = 20$ kPa, $\phi_2 = 25°$), increases up to 8 kPa from 0 kPa.

(b) Placing a stronger layer over a weaker stratum undoubtedly improves the stability of the slope and this improvement is more significant for steep slopes. For the previous example, (i) if the cohesive strength of the top layer rises from 0 to 8 kPa (keeping ϕ_1 equals to be 35°), the improvement in F_s for 25° and 45° slope occurs by 19% and 56%, respectively; and, (ii) if the frictional strength increases from 35° to 45°, F_s improves by 26% and 42% for 25° and 45° slope, respectively.

(c) When the thickness of the top layer is within a certain limit, the strength of the bottom layer also influences the stability of the slope. There is almost a linear relationship between the improvement of F_s with the increase in cohesive strength of the bottom layer. However, the relation between the improvement of F_s with the increase in frictional strength of the bottom layer is highly nonlinear.

(d) The tabulated data clearly reveals that the improvement in F_s is quite significant as the top layer thickness changes from $0.2D$ to $0.4D$. On the contrary, when t/D ratio varies from 0.6 to 0.8, the improvement in stability is almost negligible. The effect of the thickness of the top layer is further studied graphically.

Figure 2 illustrates the variation of F_s with t/D for a 25° slope. Figures 2(a) and (b) represent the cases where weaker bottom layer ($\phi_2 = 25°$) is strengthened by placing two different cohesionless layer of friction angle 40° and 45°. Figures 2(c) and (d) displays the cases where the cohesion of the top layer is considered as 8 kPa. It is quite evident that higher the strength of the top layer higher would be the safety factor, F_s. These figures depict that there is a certain t/D beyond which there is hardly any improvement in stability of the slopes. This particular top layer thickness is termed as optimum thickness

Table 1 Proposed stability chart (indicating the factor of safety) corresponding to $\varphi_2 = 20°$

φ_1	c_1 (kPa)	c_2 (kPa)	$t = 0.2D$			$t = 0.4D$			$t = 0.5D$			$t = 0.6D$			$t = 0.8D$		
			$\beta = 25°$	$\beta = 35°$	$\beta = 45°$	$\beta = 25°$	$\beta = 35°$	$\beta = 45°$	$\beta = 25°$	$\beta = 35°$	$\beta = 45°$	$\beta = 25°$	$\beta = 35°$	$\beta = 45°$	$\beta = 25°$	$\beta = 35°$	$\beta = 45°$
35°	0	5	1.074	0.782	0.603	1.224	0.903	0.683	1.354	0.996	0.675	1.504	1.001	0.694	1.504	1.001	0.694
		10	1.217	0.913	0.685	1.331	0.998	0.677	1.443	1.002	0.692	1.504	0.996	0.694	1.504	1.001	0.694
		15	1.345	1.004	0.685	1.428	1.002	0.674	1.504	1.002	0.674	1.504	0.996	0.694	1.504	0.996	0.694
		20	1.464	1.001	0.701	1.504	1.002	0.674	1.504	1.002	0.675	1.504	1.001	0.694	1.504	1.001	0.694
	5	5	1.101	0.811	0.634	1.278	0.974	0.774	1.411	1.126	0.930	1.740	1.298	0.980	1.816	1.298	0.980
		10	1.240	0.938	0.750	1.379	1.063	0.852	1.497	1.200	0.981	1.794	1.298	0.980	1.816	1.298	0.980
		15	1.365	1.049	0.851	1.475	1.143	0.921	1.577	1.264	0.981	1.821	1.298	0.980	1.816	1.298	0.980
		20	1.484	1.155	0.944	1.563	1.219	0.983	1.654	1.296	0.981	1.818	1.298	0.980	1.817	1.298	0.980
	8	5	1.114	0.827	0.649	1.306	1.007	0.812	1.438	1.162	0.978	1.777	1.409	1.084	1.943	1.409	1.084
		10	1.253	0.951	0.764	1.406	1.096	0.891	1.524	1.238	1.039	1.829	1.409	1.084	1.943	1.409	1.084
		15	1.376	1.062	0.864	1.500	1.175	0.958	1.604	1.304	1.082	1.880	1.409	1.084	1.943	1.409	1.084
		20	1.495	1.167	0.958	1.587	1.250	1.019	1.682	1.364	1.087	1.930	1.409	1.084	1.943	1.409	1.084
40°	0	5	1.091	0.796	0.615	1.282	0.959	0.732	1.455	1.152	0.841	1.803	1.194	0.828	1.803	1.199	0.831
		10	1.235	0.929	0.733	1.403	1.069	0.838	1.546	1.195	0.840	1.803	1.199	0.828	1.803	1.194	0.831
		15	1.364	1.045	0.838	1.502	1.157	0.840	1.633	1.198	0.841	1.803	1.194	0.831	1.803	1.200	0.831
		20	1.479	1.153	0.839	1.595	1.198	0.840	1.713	1.197	0.832	1.803	1.200	0.824	1.803	1.194	0.831
	5	5	1.114	0.822	0.641	1.334	1.028	0.821	1.499	1.214	1.020	1.888	1.514	1.138	2.132	1.515	1.138
		10	1.258	0.951	0.761	1.444	1.125	0.909	1.588	1.297	1.091	1.945	1.514	1.138	2.132	1.515	1.138
		15	1.383	1.064	0.864	1.541	1.211	0.984	1.674	1.372	1.138	2.003	1.514	1.138	2.132	1.515	1.138
		20	1.502	1.171	0.959	1.634	1.293	1.050	1.755	1.441	1.139	2.058	1.514	1.138	2.132	1.515	1.138
	8	5	1.128	0.837	0.658	1.363	1.058	0.857	1.523	1.245	1.060	1.919	1.631	1.247	2.269	1.632	1.247
		10	1.268	0.964	0.773	1.468	1.153	0.943	1.611	1.328	1.135	1.976	1.631	1.247	2.269	1.632	1.247
		15	1.394	1.077	0.877	1.562	1.239	1.018	1.697	1.403	1.197	2.034	1.631	1.247	2.269	1.632	1.247
		20	1.511	1.183	0.971	1.654	1.320	1.087	1.777	1.473	1.246	2.090	1.631	1.247	2.269	1.632	1.247

Table 1 (continued)

φ_1	c_1 (kPa)	c_2 (kPa)	$t = 0.2D$			$t = 0.4D$			$t = 0.5D$			$t = 0.6D$			$t = 0.8D$		
			$\beta = 25°$	$\beta = 35°$	$\beta = 45°$	$\beta = 25°$	$\beta = 35°$	$\beta = 45°$	$\beta = 25°$	$\beta = 35°$	$\beta = 45°$	$\beta = 25°$	$\beta = 35°$	$\beta = 45°$	$\beta = 25°$	$\beta = 35°$	$\beta = 45°$
45°	0	5	1.105	0.807	0.624	1.328	1.001	0.784	1.545	1.246	0.997	1.983	1.420	0.988	2.148	1.428	0.991
		10	1.253	0.942	0.749	1.468	1.132	0.897	1.639	1.235	0.993	2.046	1.428	0.991	2.148	1.428	0.991
		15	1.382	1.061	0.856	1.570	1.227	0.982	1.728	1.352	0.960	2.107	1.428	0.991	2.148	1.428	0.988
		20	1.504	1.169	0.952	1.669	1.313	0.988	1.814	1.422	0.991	2.148	1.414	0.988	2.148	1.428	0.988
	5	5	1.124	0.831	0.647	1.382	1.065	0.858	1.581	1.296	1.104	2.025	1.762	1.318	2.505	1.762	1.318
		10	1.271	0.963	0.770	1.504	1.181	0.960	1.675	1.386	1.187	2.087	1.762	1.320	2.505	1.762	1.318
		15	1.400	1.078	0.875	1.607	1.273	1.044	1.764	1.463	1.258	2.155	1.762	1.318	2.505	1.762	1.318
		20	1.520	1.186	0.973	1.701	1.361	1.117	1.848	1.544	1.317	2.215	1.762	1.318	2.505	1.762	1.320
	8	5	1.136	0.843	0.660	1.408	1.099	0.893	1.602	1.323	1.137	2.057	1.838	1.433	2.641	1.885	1.433
		10	1.282	0.973	0.781	1.524	1.207	0.992	1.694	1.411	1.220	2.119	1.887	1.433	2.641	1.885	1.433
		15	1.409	1.091	0.886	1.623	1.298	1.073	1.782	1.493	1.294	2.182	1.885	1.433	2.641	1.885	1.433
		20	1.529	1.195	0.983	1.718	1.384	1.147	1.867	1.569	1.360	2.244	1.885	1.433	2.641	1.885	1.433

Table 2 Proposed stability chart (indicating the factor of safety) corresponding to $\varphi_2 = 25°$

φ_1	c_1 (kPa)	c_2 (kPa)	$t = 0.2D$			$t = 0.4D$			$t = 0.5D$			$t = 0.6D$			$t = 0.8D$		
			$\beta = 25°$	$\beta = 35°$	$\beta = 45°$	$\beta = 25°$	$\beta = 35°$	$\beta = 45°$	$\beta = 25°$	$\beta = 35°$	$\beta = 45°$	$\beta = 25°$	$\beta = 35°$	$\beta = 45°$	$\beta = 25°$	$\beta = 35°$	$\beta = 45°$
35°	0	5	1.297	0.885	0.698	1.405	1.000	0.674	1.504	1.002	0.692	1.504	1.001	0.694	1.504	1.001	0.694
		10	1.448	1.003	0.685	1.507	1.002	0.674	1.504	1.002	0.674	1.504	1.001	0.694	1.504	1.001	0.694
		15	1.506	1.000	0.685	1.504	1.001	0.677	1.504	1.002	0.692	1.504	1.001	0.694	1.504	1.001	0.694
		20	1.506	1.000	0.695	1.507	0.998	0.700	1.504	1.002	0.691	1.504	1.001	0.694	1.504	1.001	0.694
	5	5	1.329	0.971	0.750	1.479	1.101	0.858	1.603	1.232	0.974	1.818	1.298	0.980	1.816	1.298	0.980
		10	1.477	1.100	0.870	1.579	1.185	0.931	1.682	1.287	0.983	1.818	1.298	0.980	1.816	1.298	0.980
		15	1.607	1.217	0.976	1.671	1.262	0.993	1.756	1.296	0.981	1.818	1.298	0.980	1.816	1.298	0.980
		20	1.731	1.326	1.074	1.759	1.333	1.026	1.824	1.296	0.981	1.818	1.298	0.980	1.816	1.298	0.980
	8	5	1.349	0.989	0.770	1.515	1.142	0.907	1.641	1.281	1.045	1.946	1.409	1.084	1.943	1.409	1.084
		10	1.492	1.115	0.886	1.613	1.227	0.977	1.721	1.347	1.080	1.944	1.409	1.084	1.943	1.409	1.084
		15	1.623	1.233	0.991	1.705	1.303	1.038	1.797	1.398	1.087	1.946	1.409	1.084	1.943	1.409	1.084
		20	1.746	1.340	1.089	1.791	1.374	1.098	1.868	1.406	1.085	1.946	1.409	1.084	1.943	1.409	1.084
40°	0	5	1.322	0.955	0.729	1.499	1.094	0.821	1.660	1.198	0.841	1.803	1.199	0.831	1.803	1.199	0.828
		10	1.473	1.093	0.839	1.613	1.191	0.835	1.751	1.197	0.840	1.803	1.200	0.840	1.803	1.200	0.832
		15	1.607	1.205	0.841	1.713	1.198	0.833	1.802	1.197	0.841	1.803	1.199	0.831	1.803	1.192	0.833
		20	1.734	1.200	0.841	1.802	1.198	0.839	1.803	1.199	0.840	1.803	1.199	0.828	1.803	1.200	0.832
	5	5	1.352	0.986	0.764	1.563	1.177	0.924	1.725	1.357	1.100	2.126	1.514	1.138	2.132	1.514	1.138
		10	1.498	1.120	0.886	1.667	1.269	1.003	1.811	1.430	1.139	2.138	1.514	1.138	2.132	1.515	1.138
		15	1.629	1.237	0.993	1.764	1.351	1.075	1.893	1.490	1.139	2.134	1.514	1.138	2.132	1.515	1.138
		20	1.754	1.350	1.092	1.856	1.428	1.139	1.970	1.512	1.140	2.134	1.514	1.138	2.132	1.515	1.138
	8	5	1.368	1.004	0.781	1.595	1.213	0.967	1.756	1.398	1.155	2.168	1.631	1.247	2.269	1.632	1.247
		10	1.512	1.137	0.902	1.696	1.305	1.046	1.842	1.472	1.215	2.215	1.631	1.247	2.269	1.632	1.247
		15	1.643	1.252	1.007	1.791	1.386	1.114	1.923	1.540	1.248	2.265	1.631	1.247	2.268	1.632	1.247
		20	1.766	1.360	1.107	1.884	1.464	1.181	2.000	1.597	1.247	2.269	1.631	1.247	2.268	1.633	1.247

Table 2 (continued)

φ_1	c_1 (kPa)	c_2 (kPa)	$t = 0.2D$			$t = 0.4D$			$t = 0.5D$			$t = 0.6D$			$t = 0.8D$		
			$\beta = 25°$	$\beta = 35°$	$\beta = 45°$	$\beta = 25°$	$\beta = 35°$	$\beta = 45°$	$\beta = 25°$	$\beta = 35°$	$\beta = 45°$	$\beta = 25°$	$\beta = 35°$	$\beta = 45°$	$\beta = 25°$	$\beta = 35°$	$\beta = 45°$
45°	0	5	1.555	1.166	0.925	1.726	1.313	1.036	1.890	1.498	1.116	2.212	1.531	1.115	2.211	1.533	1.112
		10	1.496	1.111	0.872	1.703	1.283	0.990	1.880	1.430	0.991	2.148	1.428	0.991	2.148	1.428	0.988
		15	1.626	1.234	0.881	1.806	1.374	0.994	1.969	1.429	0.989	2.148	1.414	0.991	2.148	1.423	0.988
		20	1.756	1.346	0.994	1.901	1.431	0.998	2.051	1.425	0.989	2.148	1.428	0.991	2.148	1.414	0.988
	5	5	1.367	1.001	0.772	1.630	1.240	0.981	1.837	1.471	1.217	2.312	1.762	1.318	2.505	1.762	1.320
		10	1.519	1.137	0.901	1.749	1.344	1.073	1.929	1.553	1.286	2.367	1.762	1.318	2.505	1.762	1.320
		15	1.653	1.257	1.008	1.848	1.433	1.152	2.008	1.628	1.320	2.422	1.762	1.318	2.505	1.762	1.320
		20	1.777	1.368	1.110	1.943	1.516	1.220	2.096	1.697	1.320	2.476	1.762	1.318	2.505	1.762	1.320
	8	5	1.381	1.016	0.789	1.663	1.277	1.021	1.864	1.506	1.264	2.344	1.885	1.433	2.641	1.885	1.433
		10	1.532	1.151	0.914	1.776	1.376	1.110	1.953	1.587	1.336	2.394	1.885	1.433	2.641	1.885	1.433
		15	1.664	1.269	1.022	1.872	1.464	1.186	2.039	1.663	1.397	2.457	1.885	1.433	2.641	1.885	1.433
		20	1.787	1.381	1.122	1.967	1.547	1.257	2.121	1.733	1.433	2.511	1.885	1.433	2.641	1.885	1.433

Table 3 Proposed stability chart (indicating the factor of safety) corresponding to $\varphi_2 = 30°$

φ_1	c_1 (kPa)	c_2 (kPa)	$t = 0.2D$			$t = 0.4D$			$t = 0.5D$			$t = 0.6D$			$t = 0.8D$		
			$\beta = 25°$	$\beta = 35°$	$\beta = 45°$	$\beta = 25°$	$\beta = 35°$	$\beta = 45°$	$\beta = 25°$	$\beta = 35°$	$\beta = 45°$	$\beta = 25°$	$\beta = 35°$	$\beta = 45°$	$\beta = 25°$	$\beta = 35°$	$\beta = 45°$
35°	0	5	1.506	1.000	0.704	1.504	1.002	0.674	1.504	1.002	0.677	1.504	0.996	0.694	1.504	1.001	0.694
		10	1.506	1.000	0.689	1.504	1.000	0.700	1.504	1.002	0.674	1.504	1.001	0.694	1.504	1.001	0.694
		15	1.506	1.000	0.685	1.506	1.000	0.662	1.504	0.997	0.676	1.504	0.996	0.694	1.504	1.001	0.694
		20	1.506	1.000	0.704	1.506	1.001	0.677	1.504	1.002	0.677	1.504	1.001	0.694	1.504	1.001	0.694
	5	5	1.566	1.130	0.865	1.658	1.205	0.924	1.746	1.283	0.983	1.818	1.298	0.980	1.816	1.298	0.980
		10	1.718	1.267	0.990	1.754	1.283	0.991	1.812	1.296	0.983	1.818	1.298	0.980	1.816	1.298	0.980
		15	1.857	1.388	1.102	1.843	1.346	1.025	1.822	1.296	0.981	1.818	1.298	0.980	1.816	1.298	0.980
		20	1.987	1.502	1.204	1.876	1.344	1.026	1.822	1.296	0.981	1.818	1.298	0.980	1.816	1.298	0.980
	8	5	1.590	1.156	0.891	1.703	1.259	0.982	1.804	1.361	1.076	1.944	1.409	1.084	1.943	1.409	1.084
		10	1.738	1.289	1.010	1.798	1.336	1.048	1.874	1.398	1.087	1.944	1.409	1.084	1.943	1.409	1.084
		15	1.875	1.405	1.121	1.888	1.407	1.105	1.936	1.407	1.085	1.944	1.409	1.084	1.943	1.409	1.084
		20	2.002	1.520	1.221	1.972	1.475	1.146	1.946	1.407	1.085	1.944	1.409	1.084	1.943	1.409	1.084
40°	0	5	1.560	1.113	0.839	1.687	1.198	0.833	1.804	1.199	0.834	1.803	1.199	0.833	1.803	1.186	0.823
		10	1.717	1.199	0.839	1.800	1.198	0.829	1.805	1.200	0.829	1.803	1.200	0.831	1.803	1.192	0.840
		15	1.805	1.198	0.841	1.802	1.198	0.835	1.803	1.197	0.840	1.803	1.200	0.824	1.803	1.199	0.828
		20	1.805	1.205	0.841	1.802	1.198	0.833	1.806	1.197	0.834	1.803	1.192	0.831	1.803	1.192	0.831
	5	5	1.574	1.131	0.862	1.727	1.248	0.942	1.868	1.367	1.002	1.984	1.370	1.002	1.985	1.370	1.002
		10	1.731	1.273	0.991	1.832	1.337	1.022	1.941	1.368	1.003	1.984	1.370	1.003	1.985	1.370	1.002
		15	1.870	1.398	1.104	1.929	1.398	1.029	1.983	1.368	1.003	1.984	1.370	1.002	1.985	1.370	1.002
		20	2.002	1.510	1.139	2.015	1.398	1.029	1.983	1.368	1.003	1.984	1.370	1.003	1.984	1.370	1.002
	8	5	1.597	1.155	0.886	1.771	1.306	1.008	1.918	1.454	1.135	2.134	1.514	1.138	2.132	1.514	1.138
		10	1.749	1.291	1.010	1.872	1.391	1.081	1.999	1.507	1.139	2.134	1.514	1.138	2.132	1.514	1.138
		15	1.888	1.414	1.124	1.967	1.472	1.147	2.075	1.512	1.140	2.134	1.514	1.138	2.132	1.515	1.138
		20	2.017	1.527	1.226	2.058	1.543	1.188	2.140	1.514	1.140	2.134	1.514	1.138	2.132	1.515	1.138

Table 3 (continued)

φ_1	c_1 (kPa)	c_2 (kPa)	$t = 0.2D$			$t = 0.4D$			$t = 0.5D$			$t = 0.6D$			$t = 0.8D$		
			$\beta = 25°$	$\beta = 35°$	$\beta = 45°$	$\beta = 25°$	$\beta = 35°$	$\beta = 45°$	$\beta = 25°$	$\beta = 35°$	$\beta = 45°$	$\beta = 25°$	$\beta = 35°$	$\beta = 45°$	$\beta = 25°$	$\beta = 35°$	$\beta = 45°$
45°	0	5	1.589	1.139	0.737	1.794	1.296	0.975	2.003	1.429	0.991	2.148	1.428	0.992	2.148	1.428	0.988
		10	1.748	1.283	0.990	1.921	1.411	0.992	2.091	1.425	1.001	2.148	1.428	0.988	2.148	1.428	0.988
		15	1.890	1.411	0.987	2.024	1.430	0.987	2.148	1.429	0.991	2.148	1.428	0.992	2.148	1.428	0.988
		20	2.022	1.428	0.987	2.120	1.427	0.988	2.148	1.429	0.996	2.148	1.428	0.988	2.148	1.428	0.988
	5	5	1.603	1.154	0.878	1.830	1.345	1.026	2.034	1.551	1.173	2.340	1.609	1.177	2.340	1.609	1.177
		10	1.760	1.297	1.011	1.946	1.444	1.113	2.120	1.610	1.175	2.340	1.609	1.177	2.340	1.609	1.177
		15	1.899	1.426	1.127	2.048	1.534	1.190	2.202	1.610	1.175	2.340	1.609	1.177	2.340	1.609	1.177
		20	2.029	1.541	1.233	2.145	1.612	1.203	2.280	1.610	1.175	2.340	1.609	1.177	2.340	1.609	1.177
	8	5	1.621	1.173	0.901	1.871	1.396	1.087	2.070	1.610	1.288	2.505	1.762	1.318	2.505	1.762	1.318
		10	1.777	1.314	1.029	1.984	1.491	1.170	2.157	1.683	1.320	2.504	1.762	1.318	2.505	1.762	1.318
		15	1.913	1.441	1.141	2.080	1.575	1.240	2.239	1.744	1.320	2.504	1.762	1.318	2.505	1.762	1.318
		20	2.043	1.553	1.249	2.177	1.655	1.309	2.319	1.759	1.319	2.504	1.762	1.318	2.505	1.762	1.318

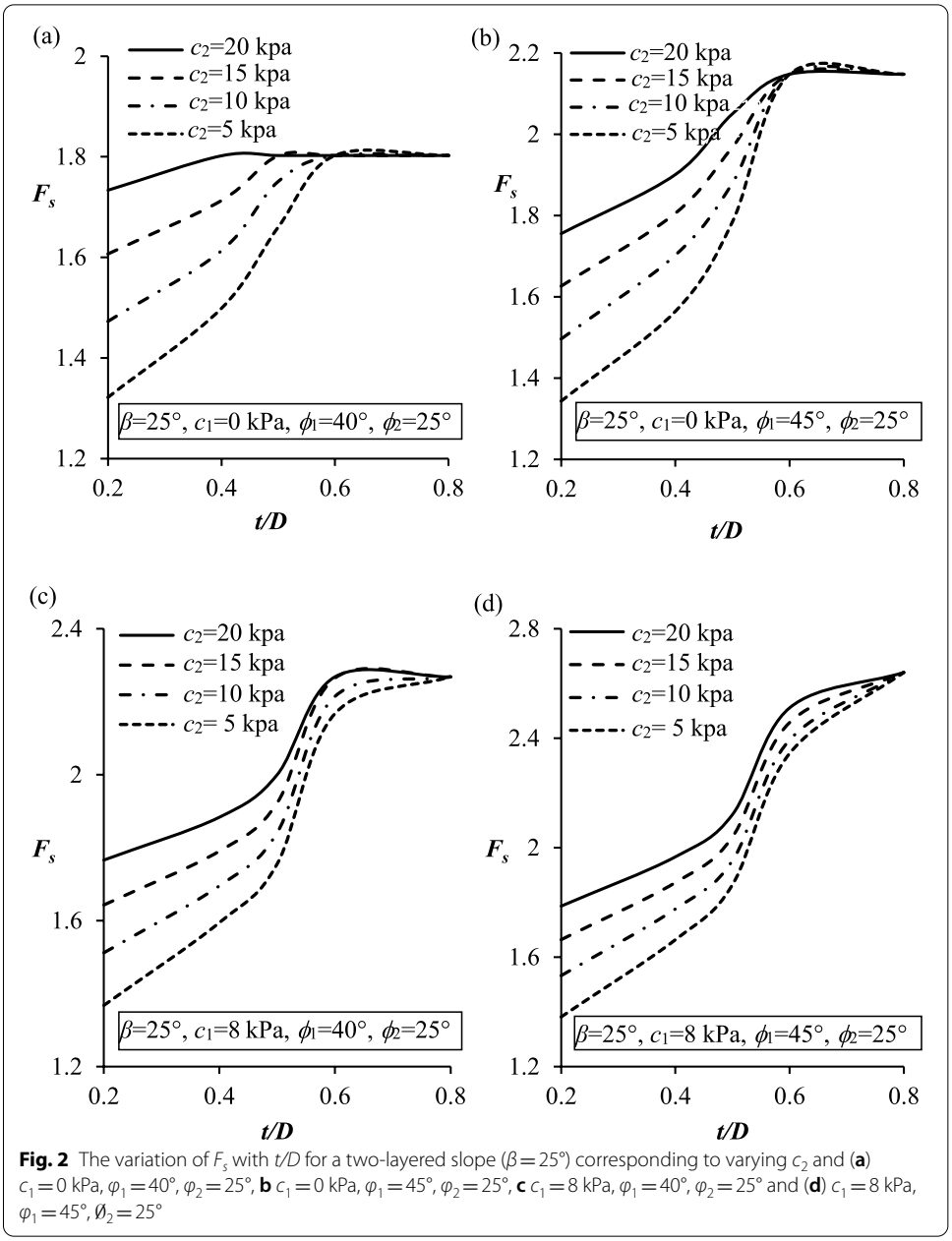

Fig. 2 The variation of F_s with t/D for a two-layered slope ($\beta = 25°$) corresponding to varying c_2 and (**a**) $c_1 = 0$ kPa, $\varphi_1 = 40°$, $\varphi_2 = 25°$, **b** $c_1 = 0$ kPa, $\varphi_1 = 45°$, $\varphi_2 = 25°$, **c** $c_1 = 8$ kPa, $\varphi_1 = 40°$, $\varphi_2 = 25°$ and (**d**) $c_1 = 8$ kPa, $\varphi_1 = 45°$, $\emptyset_2 = 25°$

and is referred here as dimensionless parameter, 't_{opt}/D'. The value of t_{opt}/D increases with the increase in the strength of the top layer. The figure shows that the dependence of t_{opt}/D on the cohesive strength of the bottom layer is further influenced by the frictional strength of the top layer; when $\phi_1 = 40°$, t_{opt}/D decreases with increase in c_2 however, when $\phi_1 = 45°$ there is no impact of c_2 on the computed value of t_{opt}/D.

Figure 3 shows the variation of F_s with t/D for $\beta = 25°$ and 45°, corresponding to two different ϕ_2, namely, 20° and 30°. The properties of the top layer are kept to be constant and the cohesive strength of the bottom layer is varied within the range of 5–20 kPa. The figures clearly reveal that for the same soil properties, optimum thickness of the top layer is significantly smaller for the steeper slopes. As the frictional strength of the bottom

layer increases, the magnitude of t_{opt}/D further reduces. The numerical solutions give an impression that the impact of the strength of the top layer on the stability is much higher than the strength of the bottom layer.

Figure 4 shows the mesh pattern at the collapse state for three different slope angles, namely, 25°, 35° and 45°. The soil profiles for these three cases are kept to be the same. It is to be noted that adaptive mesh refinement technique continuously updates the sizes of all the elements in an optimal fashion by computing the variations of stresses and velocities. Finer elements were automatically placed in the shear failure zone. Hence, these meshes indirectly depict the failure patterns. The figure shows that the size of the failure zone decreases with the increase in slope angle. Moreover, as the slope angle increases the failure is likely to become toe failure. This observation is in accordance with the studies of Lim et al. [29] and Sazzad, et al. [40] who had earlier reported that if the top layer is considered to be stronger than the bottom layer and the slope angle is considered to be less than equal to 45° the incipient state of collapse in the soil slope will be triggered by developing base failure. As the steepness of the slope increases, the extent of the failure zone seems to be restricted closer to the slope surface.

Figure 5 illustrates failure state corresponding to three different thickness of the top layer. The soil properties of the top layer as well as the bottom layer are the same for all the three cases. The figure demonstrates that as the thickness of the top layer increases the type of failure surface turns from toe to base. However, beyond a certain thickness, the slope collapses by developing the toe failure surface and the shear zone seems to be confined within the top layer. This observation substantiates the existence of t_{opt}/D.

Figure 6 depicts the mesh pattern at the collapse state corresponding to three different frictional angle of the top layer. All other geometrical and material strength parameters are kept to be the same. The figure illustrates that as the frictional strength of the top layer increases the failure zone grows in size. However, the extent at which the finer elements are laid at the collapse state goes thinner with the increase in ϕ_1. It gives an impression that the thickness of the shearing zone (i.e. shear band) becomes smaller with the placement of stronger layer over a weaker stratum.

Comparison of results

Comparisons of both the limiting solutions, for the homogenous and layered slopes, are presented in Tables 4 and 5, respectively. In most of the cases the difference seems to be in the second decimal place. Closeness of the lower and upper bound solutions further depicts the accuracy in the computed solutions. Limit theorems suggest that the true solution will lie somewhere between these bounding values. It should be recalled that the safety factors charts presented in Tables 1, 2, 3, are the average value of the two extremities.

Table 6 shows the comparison of the present solutions computed with the numerical results provided by Dawson et al. [10] for a homogenous slope of 10 m height having unit weight of soil, $\gamma = 20$ kN/m^3 and cohesion, $c = 12.38$ kPa. Dawson et al. [10] had employed strength reduction method by using the explicit finite difference code, *FLAC*. As the frictional strength of the soil increases the present method provides higher stability value. For the same soil, the difference between these two solutions reduces as the steepness of the slope increases. The reason may be attributed

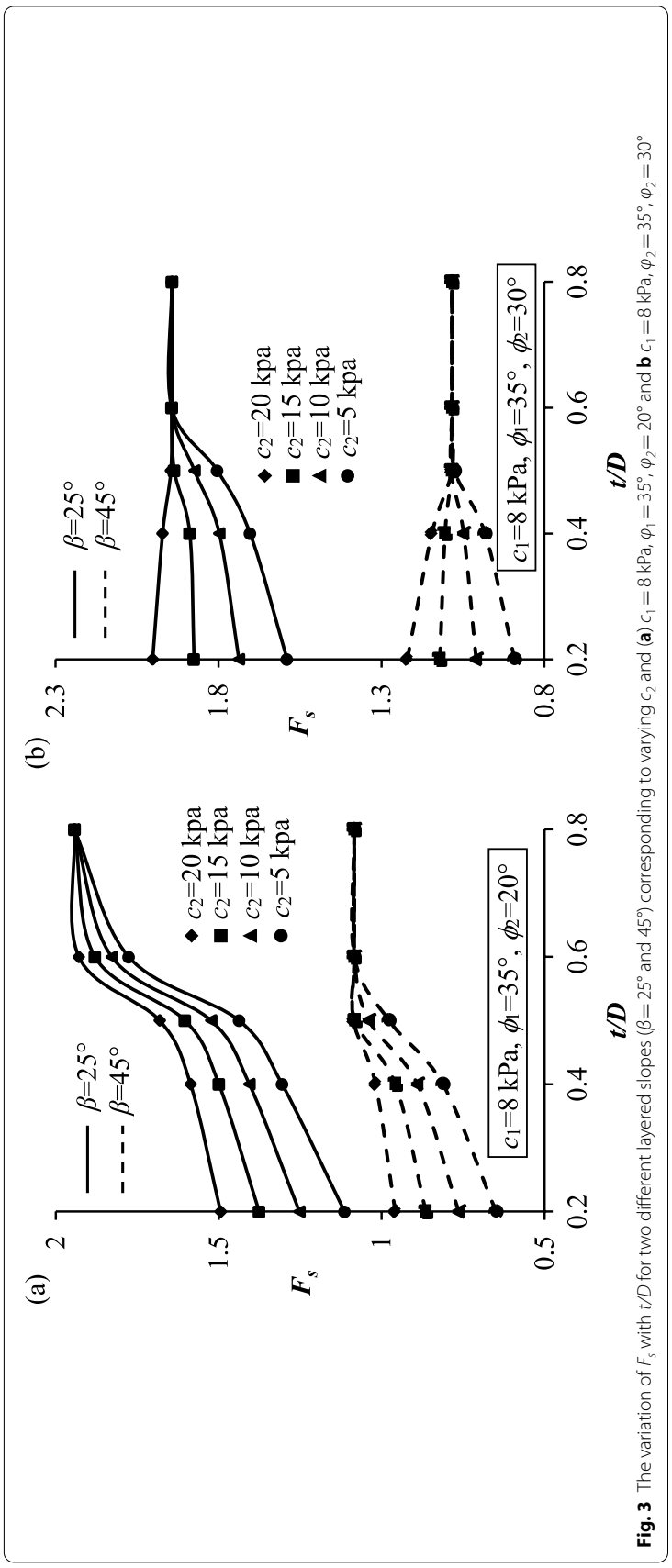

Fig. 3 The variation of F_s with t/D for two different layered slopes ($\beta = 25°$ and 45°) corresponding to varying c_2 and (**a**) $c_1 = 8$ kPa, $\varphi_1 = 35°$, $\varphi_2 = 20°$ and **b** $c_1 = 8$ kPa, $\varphi_2 = 35°$, $\varphi_2 = 30°$

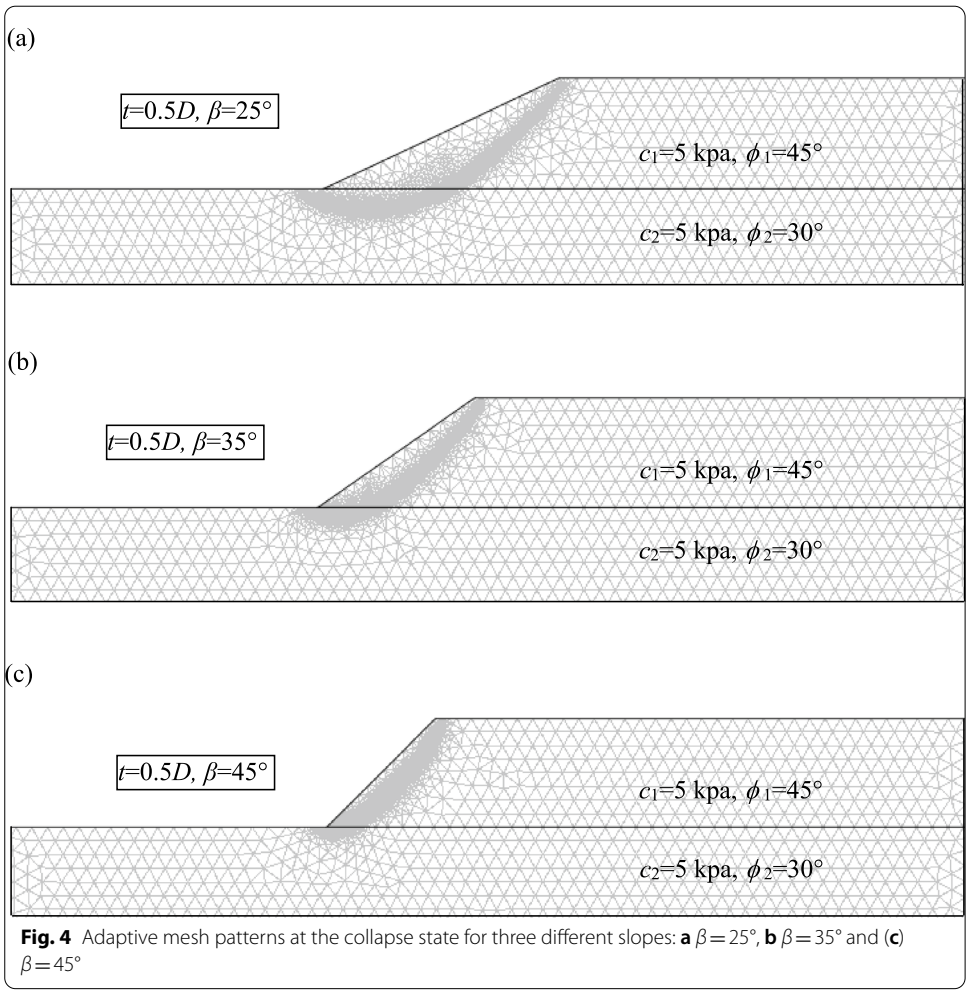

Fig. 4 Adaptive mesh patterns at the collapse state for three different slopes: **a** $\beta = 25°$, **b** $\beta = 35°$ and (**c**) $\beta = 45°$

not only to the methodology but also to the choice of elements. Dawson et al. [10] had discretized the chosen domain with four nodded rectangular elements, whereas, in the present work three nodded linear triangular elements are used. The same trend is also observed while the solutions of Dawson et al. [10] are compared with the upper bound solutions (assuming log spiral mechanism) obtained by Chen [6]. It is to be noted that the present finite element limit solutions are quite smaller than those rigid block upper bound solutions provided by Chen [6]. It shows the improvement of the solutions when finite element limit analysis is employed for the analysis.

Table 7 shows the comparison of the present solutions with the results provided by Kumar and Samui [24] by using the rigid block upper bound method considering log-spiral failure mechanism. The comparison is carried out for 45° slope corresponding to different soil layer properties and varying top layer thickness. Similar to the previous observation, it is well noted that the present solutions become quite smaller than the reported solutions of Kumar and Samui [24] as the strength of the soil layer increases.

Table 8 illustrates the comparison of current solutions with the solutions provided by Chatterjee and Krishna [5] for non-homogeneous slopes. Chatterjee and Krishna [5]

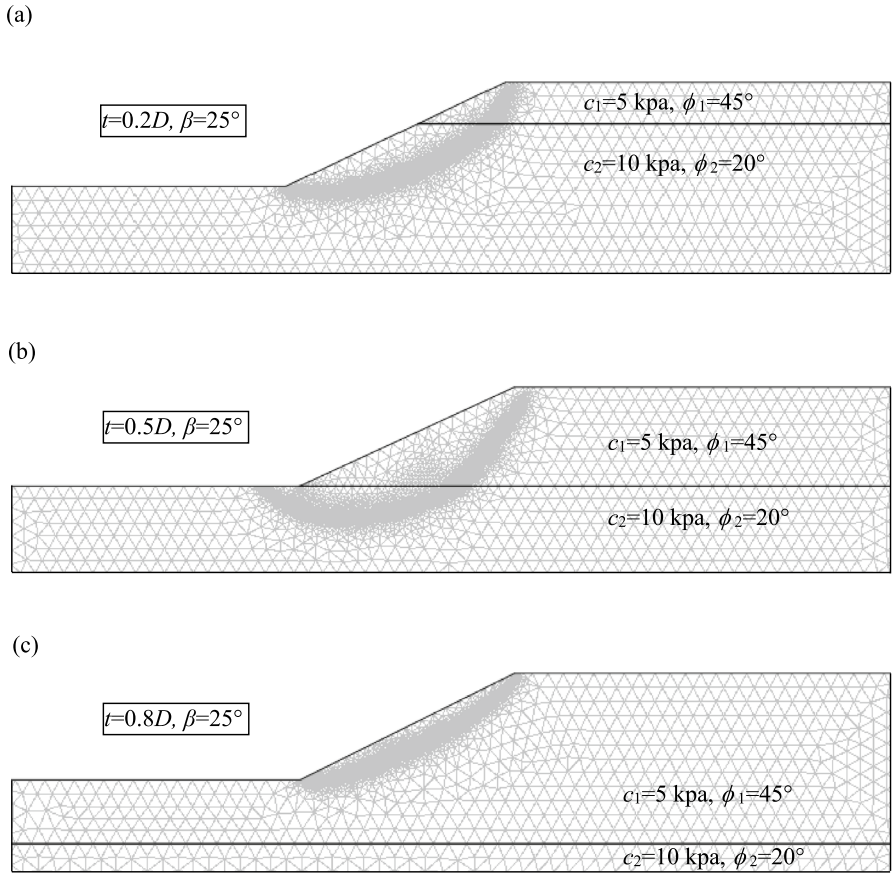

Fig. 5 Adaptive mesh patterns at the collapse state by varying the top layer thickness: **a** $t=0.2D$, **b** $t=0.5D$ and **c** $t=0.8D$

used (i) SLIDE v6 and Morgenstern and Price [33] method for performing the LEM analysis and (ii) PHASE v9 for obtaining the FE solutions. The present solutions are quite agreeable with the reported FE solutions. Table 9 depicts the comparison of present solutions with limit equilibrium solutions presented by Sazzad et al. [41] for layered soil slopes. Sazzad et al. [41] used Bishop Method [3] for LEM analysis. The present solutions appear to be smaller than the LEM solutions. This can be attributed to the fact that LEM solutions generally overestimate the factor of safety due to the usage of statical and kinematical assumptions. This is also observed in earlier studies as well [48].

Conclusions

In the present article, the stability of two-layered soil slopes is analyzed by using strength reduction method. A series of upper and lower bound limit analyses are carried out in Optum G2 software by placing different stronger layers of varied thickness over the weaker stratum. Stability charts are prepared in the form of the factor of safety for different soil properties, slope geometries and top layer thickness. The

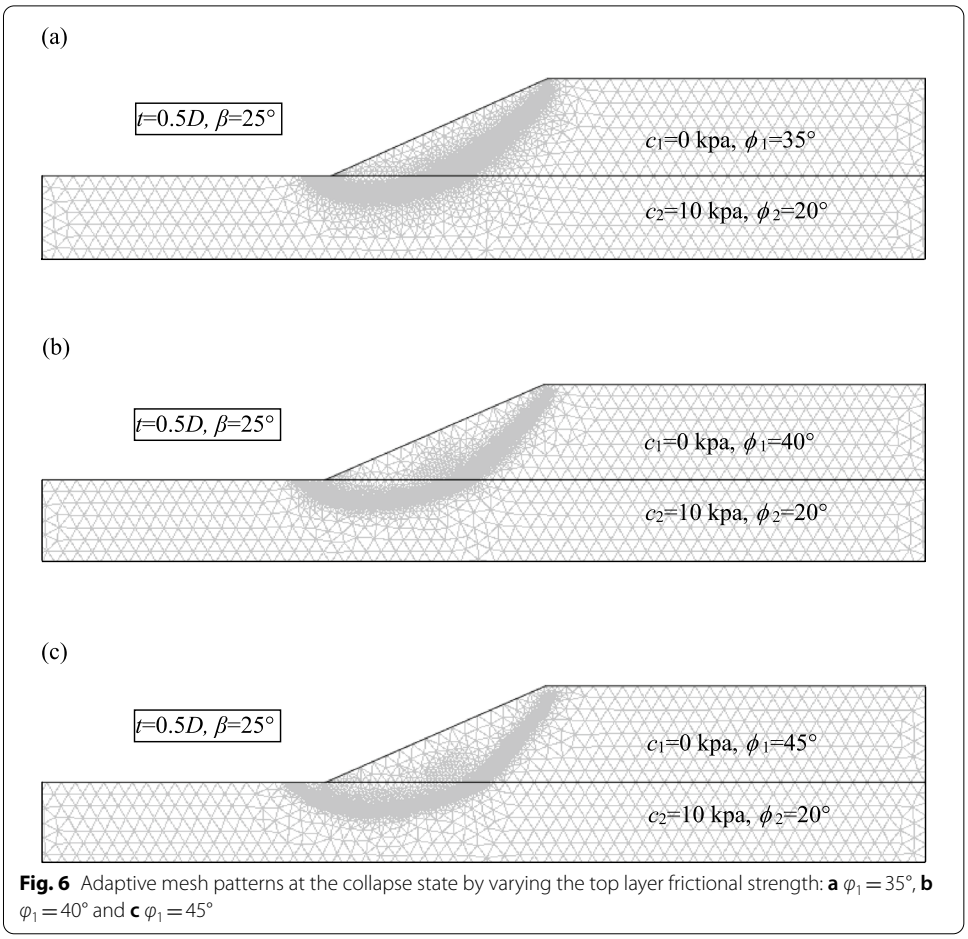

Fig. 6 Adaptive mesh patterns at the collapse state by varying the top layer frictional strength: **a** $\varphi_1 = 35°$, **b** $\varphi_1 = 40°$ and **c** $\varphi_1 = 45°$

amount of improvement in the stability by placing a layer of stronger soil over the weaker stratum is numerically investigated. The optimum thickness of the top layer is reported for a wide range of slopes. The extent and the type of the failure zones are presented for several cases. The obtained solutions compared quite well with the available solutions. The proposed design charts may be useful to the practicing engineers.

Table 4 A comparison of the computed lower and upper bound values of F_s for different homogeneous slopes

φ[a]	C[b] (kPa)	$\beta = 25°$	$\beta = 35°$	$\beta = 45°$
25°	20	1.687 (1.695)	1.292 (1.303)	1.048 (1.058)
	15	1.560 (1.566)	1.177 (1.187)	0.940 (0.951)
	10	1.419 (1.425)	1.050 (1.060)	0.827 (0.831)
	5	1.258 (1.263)	0.904 (0.913)	0.692 (0.698)

The values within and outside the parenthesis are obtained by using UB and LB method respectively

[a] φ, internal friction angle of homogeneous soil slope

[b] c, cohesion of homogeneous soil slope

Table 5 A comparison of the computed lower and upper bound values of F_s for different layered slopes

φ_1	c_1 (kPa)	c_2 (kPa)	$t = 0.2D$			$t = 0.5D$			$t = 0.8D$		
			$\beta = 25°$	$\beta = 35°$	$\beta = 45°$	$\beta = 25°$	$\beta = 35°$	$\beta = 45°$	$\beta = 25°$	$\beta = 35°$	$\beta = 45°$
45°	5	5	1.121 (1.126)	0.828 (0.834)	0.644 (0.649)	1.577 (1.584)	1.293 (1.299)	1.101 (1.107)	2.495 (2.514)	1.754 (1.769)	1.312 (1.323)
		10	1.269 (1.273)	0.959 (0.966)	0.765 (0.774)	1.671 (1.678)	1.383 (1.389)	1.184 (1.189)	2.495 (2.514)	1.754 (1.769)	1.312 (1.323)
		15	1.397 (1.402)	1.074 (1.082)	0.869 (0.880)	1.760 (1.767)	1.456 (1.470)	1.255 (1.261)	2.495 (2.514)	1.754 (1.769)	1.312 (1.323)
		20	1.515 (1.525)	1.182 (1.189)	0.967 (0.978)	1.844 (1.851)	1.541 (1.547)	1.312 (1.322)	2.495 (2.514)	1.754 (1.769)	1.312 (1.328)

The values within and outside the parenthesis are obtained by using UB and LB method respectively

Table 6 A comparison of F_s obtained by Dawson et al. [10] and Chen [6] with the present solutions for homogeneous slopes of 10 m height

β (°)	φ (°)	Present study	Dawson et al. [10][a]	Chen [6][b]
15	5	0.932	1.023	0.890
	10	1.368	1.027	2.816
30	10	0.895	1.034	0.836
	15	1.111	1.027	1.343
	20	1.330	1.033	2.552
45	10	0.701	1.019	0.576
	20	0.994	1.026	1.000
	30	1.295	1.031	2.200
	40	1.645	1.008	5.482

[a] By using the explicit finite difference code, *FLAC*

[b] By using rigid block method with an assumption of a continuous log-spiral failure mechanism

Table 7 A comparison of F_s obtained by Kumar and Samui [24] with the present solutions considering $\beta = 45°$ and $c_1 = c_2$

φ_1 (°)	φ_2 (°)	$t = \mathbf{0.4}H$		$t = \mathbf{0.6}H$	
		Present study	Kumar and Samui [24][a]	Present study	Kumar and Samui [24]
10	20	0.054	0.071	0.058	0.074
	30	0.043	0.050	0.055	0.059
	40	0.042	0.020	0.053	0.025
20	30	0.041	0.038	0.044	0.045
	40	0.034	0.014	0.041	0.017
30	40	0.032	0.012	0.034	0.013

[a] By using the rigid block upper bound method considering multi- log-spiral failure mechanism

Table 8 A comparison of F_s obtained by Chatterjee and Krishna (2018) with the present solutions considering $\beta = 26.57°$

c_1 (kPa)	φ_1 (°)	c_2 (kPa)	φ_2 (°)	$t = 0.4D$			$t = 0.5D$			$t = 0.6D$		
				Present study	Chatterjee and Krishna [5]		Present study	Chatterjee and Krishna [5]		Present study	Chatterjee and Krishna [5]	
					LEM-MP[a]	SRM[b]		LEM-MP	SRM		LEM-MP	SRM
10	30	0	36	1.46	1.747	1.65	1.57	1.790	1.66	1.67	1.790	1.69
		25	18	1.55	1.603	1.55	1.62	1.673	1.63	1.67	1.790	1.68
0	36	10	30	1.46	1.594	1.51	1.45	1.591	1.50	1.45	1.591	1.50
25	18			1.62	1.705	1.64	1.52	1.643	1.55	1.51	1.593	1.51

[a] LEM-MP, Limit equilibrium method (Morgenstern and Price)

[b] SRM, Strength reduction method

Table 9 A comparison of F_s obtained by Sazzad et al. [41] with the present solutions considering $\varphi_1 = \varphi_2 = 0°$ and $\beta = 45°$

c_2/c_1	Present study	Sazzad et al. [41][a]
0.2	0.34	0.50
0.4	0.56	0.78
0.6	0.77	0.88
0.8	0.97	1.18
1.0	1.17	1.38
1.2	1.36	1.40
1.4	1.36	1.40
1.6	1.36	1.40
1.8	1.36	1.40

[a] By using LEM-Bishop Method [3]

Acknowledgements
The corresponding author acknowledges the support of "Department of Science and Technology (DST), Government of India" under Grant Number DST/INSPIRE/04/2016/001692.

Authors' contributions
Both authors contributed to slope stability analysis and drafted this manuscript. Both authors read and approved the final manuscript.

Declarations

Competing interests
The authors declare that they have no competing interests.

Received: 6 June 2020 Accepted: 4 April 2021
Published online: 04 September 2021

References

1. Baker R, Shukha R, Operstein V, Frydman S (2006) Stability charts for pseudo-static slope stability analysis. Soil Dyn Earthq Eng 26(9):813–823
2. Binesh SM, Raei S (2014) Upper bound limit analysis of cohesive soils using mesh-free method. Geomechanics and Geoengineering 9(4):265–278
3. Bishop AW (1955) The use of the slip circle in the stability analysis of slopes. Geotechnique 5(1):7–17
4. Carrión M, Vargas EA, Velloso RQ, Farfan AD (2017) Slope stability analysis in 3D using numerical limit analysis (NLA) and elasto-plastic analysis (EPA). Geomech Geoeng 12(4):250–265
5. Chatterjee D, Murali Krishna A (2018) Stability analysis of two-layered non-homogeneous slopes. Int J Geotech Eng. 15:1–7
6. Chen WF (1975) Limit analysis and soil plasticity. Elsevier, Amsterdam
7. Chen WF, Snitbhan N, Fang HY (1975) Stability of slopes in anisotropic, nonhomogeneous soils. Can Geotech J 12(1):146–152
8. Chen ZY, Morgenstern NR (1983) Extensions to the generalized method of slices for stability analysis. Can Geotech J 20(1):104–119
9. Cheng YM, Lansivaara T, Wei WB (2007) Two-dimensional slope stability analysis by limit equilibrium and strength reduction methods. Comput Geotech 34(3):137–150
10. Dawson EM, Roth WH, Drescher A (1999) Slope stability analysis by strength reduction. Geotechnique 49(6):835–840
11. Duncan JM (1996) State of the art: limit equilibrium and finite-element analysis of slopes. J Geotech Eng 122(7):577–596
12. Fellenius W (1936) Calculation of stability of earth dam. In Transactions. 2nd Congress Large Dams. Washington, DC 4:445–462
13. Fu W, Liao Y (2010) Non-linear shear strength reduction technique in slope stability calculation. Comput Geotech 37(3):288–298
14. Gens A, Hutchinson JN, Cavounidis S (1988) Three-dimensional analysis of slides in cohesive soils. Geotechnique 38(1):1–23
15. Griffiths DV, Lane PA (1999) Slope stability analysis by finite elements. Geotechnique 49(3):387–403
16. Griffiths DV, Marquez RM (2007) Three-dimensional slope stability analysis by elasto-plastic finite elements. Geotechnique 57(6):537–546
17. Hammouri NA, Malkawi AIH, Yamin MM (2008) Stability analysis of slopes using the finite element method and limiting equilibrium approach. Bull Eng Geol Env 67(4):471–478

18. Han CY, Chen JJ, Xia XH, Wang JH (2014) Three-dimensional stability analysis of anisotropic and non-homogeneous slopes using limit analysis. J Central South Univ 21(3):1142–1147
19. Janbu N (1954) Application of composite slip surface for stability analysis. Proc Eur Conference Stability Earth Slopes Sweden 3:43–49
20. Kazemian T, Arvin MR (2019) Three-dimensional stability of locally loaded geocell-reinforced slopes by strength reduction method. Geomech Geoeng. pp. 1–17
21. Kim J, Salgado R, Yu HS (1999) Limit analysis of soil slopes subjected to pore-water pressures. J Geotech Geoenviron Eng 125(1):49–58
22. Krabbenhoft K, Lyamin AV (2015) Strength reduction finite-element limit analysis. Géotechnique Letters 5(4):250–253
23. Krahn J (2003) The 2001 RM Hardy Lecture: the limits of limit equilibrium analyses. Can Geotech J 40(3):643–660
24. Kumar J, Samui P (2006) Stability determination for layered soil slopes using the upper bound limit analysis. Geotech Geol Eng 24(6):1803–1819
25. Lane PA, Griffiths DV (2000) Assessment of stability of slopes under drawdown conditions. J Geotech Geoenviron Eng 126(5):443–450
26. Lechman JB, Griffiths DV (2000) Analysis of the progression of failure of earth slopes by finite elements. In: Griffiths DV et al., editors. Slope stability 2000 –proceedings of sessions of geo-Denver 250–265.
27. Li AJ, Merifield RS, Lyamin AV (2009) Limit analysis solutions for three dimensional undrained slopes. Comput Geotech 36(8):1330–1351
28. Li AJ, Merifield RS, Lyamin AV (2010) Three-dimensional stability charts for slopes based on limit analysis methods. Can Geotech J 47(12):1316–1334
29. Lim K, Li AJ, Lyamin AV (2015) Three-dimensional slope stability assessment of two-layered undrained clay. Comput Geotech 70:1–17
30. Liu ZQ, Zhou CY, Dong LG, Tan XS, Deng YM (2005) Slope stability and strengthening analysis by strength reduction FEM. Yantu Lixue (Rock Soil Mech) 26(4):558–561
31. Matsui T, San KC (1992) Finite element slope stability analysis by shear strength reduction technique. Soils Found 32(1):59–70
32. Michalowski RL (2002) Stability charts for uniform slopes. J Geotech Geoenviron Eng 128(4):351–355
33. Morgenstern NU, Price VE (1965) The analysis of the stability of general slip surfaces. Geotechnique 15(1):79–93
34. Naylor DJ (1981) Finite elements and slope stability. Proceedings of the NATO Advanced Study Institute, Lisbon, Portugal, Numerecical Methods in Geomechanics. pp 229–244
35. Ni P, Wang S, Zhang S, Mei L (2016) Response of heterogeneous slopes to increased surcharge load. Comput Geotech 78:99–109
36. Optum G2, Version: 2018.06.08 (academic license) Optum Computational Engineering, Copenhagen, Denmark.
37. Qian ZG, Li AJ, Merifield RS, Lyamin AV (2014) Slope stability charts for two-layered purely cohesive soils based on finite-element limit analysis methods. Int J Geomech 15(3):1–14
38. Sarkar S, Chakraborty M (2019) Pseudostatic Slope stability analysis in two-layered soil by using variational method. Earthquake Geotechnical Engineering for Protection and Development of Environment and Constructions (7th ICEGE, Rome) 4857–4864.
39. Sarma SK (1973) Stability analysis of embankments and slopes. Geotechnique 23(3):423–433
40. Sazzad MM, Moni MM (2017) Stability analysis of slopes for homogeneous and layered soil by FEM. J Eng Sci 08(1):51–62
41. Sazzad MM, Mazumder S, Moni MM (2015) Seismic stability analysis of homogeneous and layered soil slopes by LEM. Int J Comput Appl 117(22):17
42. Shiau JS, Merifield RS, Lyamin AV, Sloan SW (2011) Undrained stability of footings on slopes. Int J Geomech 11(5):381–390
43. Sloan SW (2011) Geotechnical stability analysis. Géotechnique 63(7):531–571
44. Spencer E (1967) A method of analysis of the stability of embankments assuming parallel inter-slice forces. Geotechnique 17(1):11–26
45. Sternik K (2013) Comparison of slope stability predictions by gravity increase and shear strength reduction methods. Czasopismo Techniczne. Środowisko 110(1-S):121–130
46. Taylor DW (1937) Stability of earth slopes. J Boston Soc Civil Engineers 24(3):197–247
47. Tschuchnigg F, Schweiger HF, Sloan SW (2015) Slope stability analysis by means of finite element limit analysis and finite element strength reduction techniques. Part I: numerical studies considering non-associated plasticity. Comput Geotech 70:169–177
48. Yu HS, Salgado R, Sloan SW, Kim JM (1998) Limit analysis versus limit equilibrium for slope stability. J Geotech Geoenviron Eng 124(1):1–11
49. Zaki A (1999) Slope stability analysis overview. University of Toronto, Toronto
50. Zhao SY, Zheng YR, Zhang YF (2005) Study on slope failure criterion in strength reduction finite element method. Rock Soil Mech 2:332–336
51. Zheng H, Sun G, Liu D (2009) A practical procedure for searching critical slip surfaces of slopes based on the strength reduction technique. Comput Geotech 36(1–2):1–5
52. Zienkiewicz OC, Humpheson C, Lewis RW (1975) Associated and nonassociated visco-plasticity and plasticity in soil mechanics. Geotechnique 25(4):671–689

Publisher's Note

Springer Nature remains neutral with regard to jurisdictional claims in published maps and institutional affiliations.